1995

The Effect of Current and Nickel Nitrate Concentration on the Deposition of Nickel Hydroxide Films

Christopher C. Streinz
University of South Carolina - Columbia

Andrew P. Hartman
University of South Carolina - Columbia

Sathya Motupally
University of South Carolina - Columbia

John W. Weidner
University of South Carolina - Columbia, weidner@engr.sc.edu

Publication Info

Journal of the Electrochemical Society, 1995, pages 1084-1089.

Publisher's link: http://dx.doi.org/10.1149/1.2044134
DOI: 10.1149/1.2044134

27. W. Vielstich, P. A. Christensen, S. A. Weeks, and A. Hamnett, *J. Electroanal. Chem.*, **242,** 327 (1988).
28. P. A. Christensen, A. Hamnett, and S. A. Weeks, *ibid.*, **250,** 127 (1988).
29. B. D. McNicol, *ibid.*, **118,** 71 (1981).
30. J. B. Goodenough and R. Manoharan, *Chemistry of Materials,* **1,** 391 (1989).
31. A. Hamnett, B. J. Kennedy, and F. E. Wagner, *J. Catal.*, **124,** 30 (1990).
32. J. B. Goodenough, A. Hamnett, B. J. Kennedy, R. Manoharan, and S. A. Weeks, *J. Electroanal. Chem.*, **240,** 133 (1988).
33. B. D. McNichol and R. T. Short, *ibid.*, **92,** 115 (1978).
34. M. M. P. Janssen and J. Moolhuysen, *Electrochim. Acta,* **21,** 869 (1976).
35. B. D. McNichol and R. T. Short, *J. Electroanal. Chem.*, **81,** 249 (1977).
36. H. A. Gasteiger, N. Markovic, P. N. Ross, Jr., and E. J. Cairns, *J. Phys. Chem.*, **97,** 12,020 (1993); H. A. Gasteiger, N. Markovic, P. N. Ross, Jr., and E. J. Cairns, Abstract 623, p. 990, The Electrochemical Society Extended Abstracts, Vol. 94-1, San Francisco, CA, May 22-27, 1994.
37. K. Kinoshita and P. Stonehart, in *Modern Aspects of Electrochemistry,* **12,** 183 (1977).
38. B. R. Rauhe, Jr., F. R. McLarnon, and E. J. Cairns, Lawrence Berkeley Laboratory Report No. LBL-32137 (1992).
39. D. T. Schwartz and R. H. Muller, *Surf. Sci.*, **248,** 349 (1991).
40. S. T. Mayer and R. H. Muller, *This Journal,* **139,** 426 (1992).
41. T. C. Chieu and M. S. Dresselhaus, *Phys. Rev. B*, **26,** 5867 (1982).
42. F. Tuinstra and J. L. Koenig, *J. Composite Materials,* **4,** 492 (1970).
43. J. W. Ager III, D. K. Veirs, J. Shamir, and G. M. Rosenblatt, *J. Appl. Phys.*, **66,** 3598 (1990).
44. E. J. Cairns, *Electrochem. Tech.*, **5,** 8 (1967).
45. K. A. Striebel, F. R. McLarnon, and E. J. Cairns, *This Journal,* **137,** 3351 (1990).
46. K. A. Striebel, F. R. McLarnon, and E. J. Cairns, *ibid.*, **137,** 3360 (1990).
47. K. A. Striebel, F. R. McLarnon, and E. J. Cairns, Lawrence Berkeley Laboratory Report No. LBL-24340 (1987).
48. B. D. Cullity, *Elements of X-Ray Diffraction,* 2nd ed., Addison-Wesley Pub. Co., Inc., Reading, MA (1978).
49. P. N. Ross, K. Kinoshita, A. J. Scarpellino, and P. Stonehart, *J. Electroanal. Chem.*, **63,** 97 (1975).
50. P. N. Ross, *Electrochim. Acta,* **36,** 2053 (1991).
51. K. Kinoshita and P. N. Ross, *J. Electroanal. Chem.*, **78,** 313 (1977).
52. B. Beden, F. Kadirgan, C. Lamy, and J. M. Leger, *ibid.*, **127,** 75 (1981).
53. E. Ticanelli, J. G. Beery, M. T. Paffett, and S. Gottesfeld, *ibid.*, **258,** 61 (1989).
54. P. Stonehart, *Ber. Bunsenges. Phys. Chem.*, **94,** 913 (1990).
55. S. Sarangapani, P. Lessner, M. Manoukian, J. Kosek, T. Bombard, and J. Giner, Report No. US-DOE SBIR P, 1 (1990); J. S. Kosek, S. Sarangapani, and J. Giner, Abstract 38, p. 37, The Electrochemical Society Extended Abstracts, Vol. 92-1, St. Louis, MO, May 17-21, 1992.
56. D. A. Landsman and F. J. Luczak, *Investigation of the In Situ Oxidation of Methanol in Fuel Cells,* Prepared for U.S. Army Mobility Equipment Research and Development Command, Fort Belvoir, VA, by United Technologies Power Systems (1981).
57. D. S. Cameron, G. A. Hards, B. Harrison, and R. J. Potter, *Platinum Metals Rev.*, **31,** 173 (1987).
58. J. B. Goodenough, A. Hamnett, B. J. Kennedy, R. Manoharan, and S. A. Weeks, *Electrochim. Acta,* **35,** 199 (1990).
59. A. Hamnett, S. A. Weeks, B. J. Kennedy, G. Troughton, and P. A. Christensen, *Ber. Bunsenges. Phys. Chem.*, **94,** 1014 (1990).

The Effect of Current and Nickel Nitrate Concentration on the Deposition of Nickel Hydroxide Films

Christopher C. Streinz, Andrew P. Hartman, Sathya Motupally,* and John W. Weidner**

Department of Chemical Engineering, University of South Carolina, Columbia, South Carolina 29208

ABSTRACT

An electrochemical quartz crystal nanobalance (EQCN) has been utilized to measure the mass of $Ni(OH)_2$ films electrochemically deposited from $Ni(NO_3)_2$ solutions. The objective of this work was to quantify electrochemical deposition as a function of deposition conditions. The changing mass recorded on the EQCN was demonstrated to be the result of $Ni(OH)_2$ deposition. Deposited mass was observed to increase proportionally with applied charge as suggested by previous investigators. Most significantly, the rate of deposition was found to decrease more than an order of magnitude as the $Ni(NO_3)_2$ concentration increased from 0.2 to 2.0*M*. The effect of concentration is shown to be related to Ni(II) concentration as opposed to solution pH or NO_3^- concentration. An empirical correlation is given to predict deposition rates in solutions ranging from 0.1 to 3.0*M* $Ni(NO_3)_2$ and at current densities ranging from 0.5 to 5.0 mA/cm^2. The decreased deposition rates in concentrated $Ni(NO_3)_2$ are attributed to the formation of intermediate species [*e.g.*, $NiOH^+$ or $Ni_4(OH)_4^{4+}$] which diffuse away from the reaction interface before deposition can occur.

Introduction

Nickel hydroxide is one of the most commonly used active materials for the positive electrode in rechargeable batteries. It has been shown that the electrochemical impregnation of porous nickel plaques produces superior electrodes compared to those made by the conventional loading process (see Gross for a review of electrochemical impregnation[1]). The ability to tightly control the operating conditions of the deposition process is one reason for superior performance. In electrochemical impregnation, a nickel plaque is cathodically polarized in a nickel nitrate solution. Nitrate is reduced according to the following reaction[2-6]

$$NO_3^- + 6H_2O + 8e^- \rightarrow NH_3 + 9OH^- \quad [1]$$

Other reactions have been shown to occur, but like the above reaction they also produce OH^- ions in approximately a 1:1 ratio of e^- to OH^-.[1,7,8] The production of OH^- increases the local pH, resulting in the precipitation of $Ni(OH)_2$ according to reaction 2[3-8]

$$Ni^{++} + 2OH^- \rightarrow Ni(OH)_2\downarrow \quad [2]$$

where $\log K_{sp} = -13.79$.[5]

* Electrochemical Society Student Member.
** Electrochemical Society Active Member.

In order to quantify electrochemical impregnation, Ho and Jorné[5] modeled the impregnation process under various flow configurations. However, since the mechanism for deposition is not well understood, a quantitative relationship between deposition conditions (*e.g.*, current, time, solution composition) and the mass deposited is not available. While numerous investigators have studied plaque impregnation,[1,7,9,10] relatively few have quantified the fundamental deposition chemistry using planar electrodes. Fischer[11] studied the kinetics of $Ni(OH)_2$ formation at the surface of a rotating-disk electrode as a function of current density, solution composition, and the thickness of the diffusion layer. MacArthur[12] studied the thickness of deposited films as a necessary first step in determining the diffusion coefficient of protons. He used Faraday's law to predict film thickness as a function of current and deposition time, but provided no experimental verification of film thickness other than electrochemical capacity. It will be shown in this study that MacArthur's assumption was good only at low $Ni(NO_3)_2$ concentrations. At high concentrations, film thickness is overestimated by more than an order of magnitude using Faraday's law. Corrigan *et al.*[8,13-16] have correlated various deposition conditions [all in 0.1*M* $Ni(NO_3)_2$] to film thickness on planar electrodes but have not quantitatively related deposition conditions to deposited thickness.

A few researchers have reported on the utilization of the quartz crystal microbalance to study the mass changes in nickel hydroxide films.[17-19] Of particular interest, Cordoba-Torresi *et al.*[18] observed that the mass increased approximately linearly with time (up to 250 s) during galvanostatic deposition of a $Ni(OH)_2$ film at 0.3 mA/cm^2 from a 0.01*M* $Ni(NO_3)_2$ solution. Assuming a ratio of 10 OH^-:8 e^- in the reduction of NO_3^- (see also Ref. 13-16), they calculated a deposition efficiency equal to 86%.

The objective of this study has been to use the electrochemical quartz crystal nanobalance (EQCN) to quantify the electrochemical deposition of $Ni(OH)_2$ films as a function of operating conditions (*e.g.*, time, current, solution concentration). The sensitivity of the EQCN is 1 nanogram, allowing precise *in situ* mass measurements. Quantifying the deposited mass is of interest for several reasons. First, the capacity is needed in order to correlate experimental discharge data with cell discharge models.[20] Second, accurate determinations of mass, and subsequently film thickness, are needed in order to calculate the diffusion coefficient of protons from electrochemical impedance spectroscopy data.[21] Finally, our goal has been to better describe the deposition process on planar electrodes so that impregnation of porous plaques may be more thoroughly and fundamentally modeled.

Experimental

An electrochemical quartz crystal nanobalance (EQCN, Elchema Model EQCN-501) was utilized to make *in situ* measurements of the mass deposited on a planar gold electrode during cathodic chronopotentiometry in nickel nitrate solutions. An illustration of the EQCN cell configuration can be seen in Fig. 1. As shown, the working electrode consists of a quartz crystal with a thin layer of gold sputtered on both sides. The electrode area exposed to solution during deposition is 0.2 cm^2. The resonant frequency of the reference crystal is 10.000 MHz. The EQCN has a frequency resolution of 1 Hz which corresponds to 1.1 ng mass change.[22] A Pine Model AFRDE5 bi-potentiostat was used for all current and potential control. All potentials are referenced with respect to the saturated calomel electrode (SCE), with the exception of those in Fig. 2 which are with respect to Ag/AgCl. The counterelectrode consisted of a platinum screen.

Depositions were carried out in $Ni(NO_3)_2$ solutions, whose concentrations ranged from 0.01 to 3.0*M* at applied current values ranging from 0.01 to 1.0 mA. For solution concentrations below 0.2*M* $Ni(NO_3)_2$, additional $NaNO_3$ was added such that the NO_3^- concentration was 0.4*M*. All solutions consisted of 50/50 volume percent (v/o) ethanol and water.[3,23,24] All depositions were carried out at room temperature (23 to 25°C) in order that the fundamental deposition chemistry might be more readily understood. The solution pH was found to be a function of $Ni(NO_3)_2$ concentration, ranging from 2.4 for 2.0*M* solution to 4.0 for 0.1*M* solution. In order to determine the effect of pH on deposition rate a solution containing 0.2*M* $Ni(NO_3)_2$ was acidified to solution pHs of 3.0, 2.5, 2.0, and 1.5 using nitric acid. In addition, a solution containing 2.0*M* $Ni(NO_3)_2$ was basified to pH 4.0 using concentrated KOH. Depositions were carried out in these solutions at an applied current of 0.5 mA and the data compared to that for the nonacidified or basified solutions. Additional depositions were carried out in solutions saturated in NO_3^- (obtained by adding excess $NaNO_3$) to determine the role of NO_3^- in deposition.

Finally, in order to ensure that the EQCN measured $Ni(OH)_2$ deposition, and not the deposition of metallic Ni, selected films were cycled and discharged in 3% KOH. The cyclic voltammograms were checked for the charge and discharge peaks characteristic of the $Ni(OH)_2$/NiOOH system. Further, the discharged capacity was converted to mass via Faraday's law assuming a one-electron transfer.[3] These were compared to the masses recorded on the EQCN.

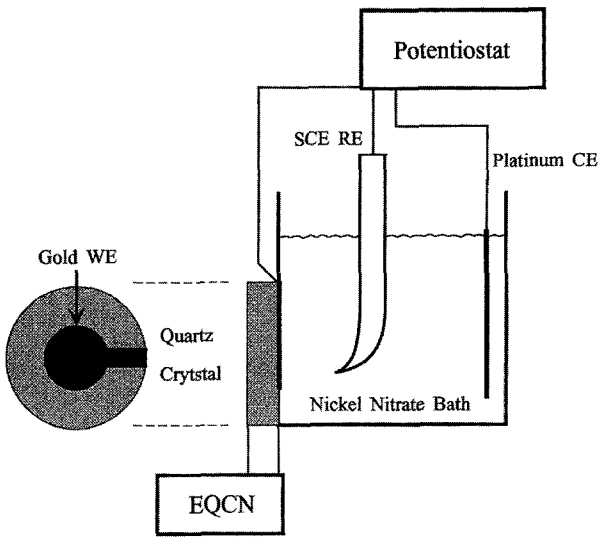

Fig. 1. An illustration of the EQCN cell configuration. The working electrode consists of a quartz crystal, sputtered with a thin layer of gold on both sides. The electrode area exposed to solution is 0.2 cm^2.

Results and Discussion

The cyclic voltammetry behavior of a 30 μg film deposited in the EQCN is illustrated in Fig. 2a (scan rate 10 mA/s). The characteristic charge and discharge peaks are readily observed indicating the presence of the $Ni(OH)_2$/NiOOH couple. The discharge behavior of the film at a constant current of 10 μA is shown in Fig. 2b. The charge passed during the galvanostatic discharge of the film is consistent with a 30 μg film, assuming a one-electron discharge process.[3] In every case in which a deposited film was cycled and discharged, cyclic voltammograms and discharge times were consistent with the masses determined via the EQCN. The physical appearance of the deposit provided further evidence for the deposition of $Ni(OH)_2$. The freshly deposited films were transparent and green, giving the QCN crystal a greenish gold appearance. A Ni deposit would be expected to appear metallic. With charging the films became black, consistent with the formation of NiOOH from $Ni(OH)_2$.[15]

A plot of mass *vs.* time for deposition in 0.2*M* $Ni(NO_3)_2$ at applied currents of 0.05, 0.1, 0.25, and 0.5 mA (0.25, 0.5, 1.25, and 2.5 mA/cm^2) is shown in Fig. 3. (The mass *vs.* time curves given in this paper are reproducible within a relative error of 5%.) The mass of the deposit increased linearly with time (with regression values, R^2, consistently greater than 0.999) indicating a constant rate of deposition. Lin-

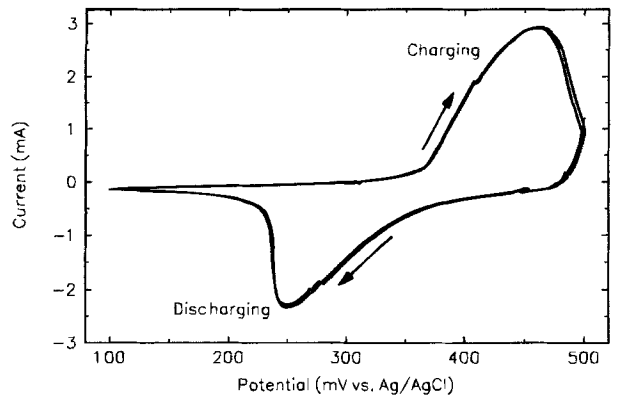

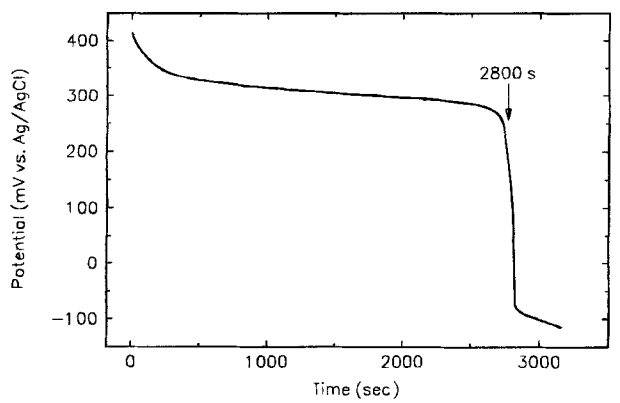

Fig. 2. (a, top) A typical cyclic voltammogram (scan rate 10 mV/s) for a 30 μg film deposited in the EQCN cell. The charge and discharge peaks are characteristic of the $Ni(OH)_2/NiOOH$ couple. (b, bottom) The typical voltage-time behavior for a 10 μA discharge of a 30 μg film. The charge passed in the discharge corresponds well to a 30 μg film, assuming a one-electron discharge reaction.

early increasing mass was observed at all deposition conditions with the exception of very low solution concentrations at high currents (*e.g.*, 0.01*M* at 0.5 mA). Deposition in dilute $Ni(NO_3)_2$ solutions is discussed later in this paper. The effect of applied current can also be observed in Fig. 3. Increasing current was observed to increase the deposition rate as indicated by the increasing slopes in the figure.

The effect of applied current is seen more clearly in Fig. 4 which is a plot of deposition rate (*i.e.*, the slope of the lines in Fig. 3) *vs.* applied current in 0.2*M* $Ni(NO_3)_2$. Note that the deposition rate increases proportionally with applied current over two orders of magnitude of current values. Figures 3 and 4 essentially show that deposited mass is proportional to charge (current × time). Since charge is a direct

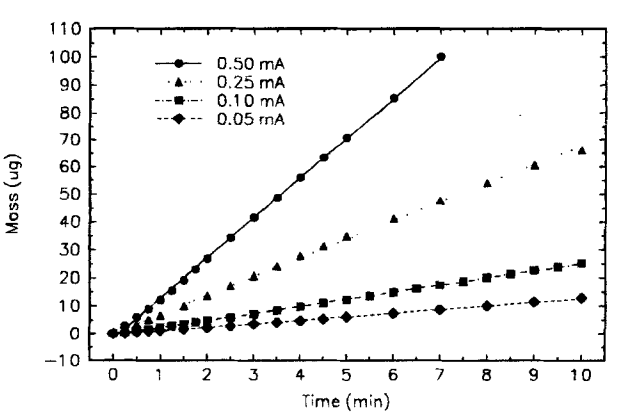

Fig. 3. A plot of mass *vs.* time for deposition in 0.2*M* $Ni(NO_3)_2$ at applied currents of 0.05, 0.1, 0.25, and 0.5 mA (0.25, 0.5, 1.25, and 2.5 mA/cm²). Note the linearly increasing mass with deposition time.

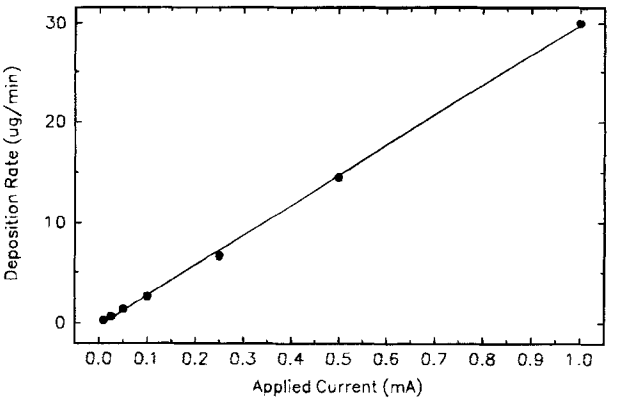

Fig. 4. A plot of deposition rate *vs.* applied current in 0.2*M* $Ni(NO_3)_2$. The deposition rate increases proportionally with current over two orders of magnitude of current values (0.01 to 1.0 mA).

measure of the production of OH^- (according to Eq. 1), Fig. 3 and 4 also show that deposited mass is proportional to OH^- generation. This is consistent with MacArthur[12] who used Faraday's law to predict the thickness of films deposited from 0.1*M* $Ni(NO_3)_2$. Our results (which are discussed in more detail below) show that this is a good approach at low concentrations (*e.g.*, 0.2*M*), however, at higher concentrations (*e.g.*, 2.0*M*) it dramatically overestimates the mass of the deposit.

The effect of solution concentration on the deposition rate is illustrated in Fig. 5, which plots mass *vs.* deposition time in several solution concentrations at 0.5 mA (2.5 mA/cm²). As discussed previously the mass is observed to increase linearly with time at each solution concentration. Note, however, that the rate of deposition (slope of the mass-time curve) increases with decreasing $Ni(NO_3)_2$ concentration. The deposition rates at each concentration are indicated on the figure. Similar behavior (increasing rate with decreasing concentration) was observed at other current values (0.1, 0.25, and 1.0 mA).

In order to separate the effect of Ni(II) and NO_3^- at high $Ni(NO_3)_2$ concentrations, deposition was measured in 0.2*M* $Ni(NO_3)_2$ saturated with $NaNO_3$. Mass *vs.* time in a 0.5 mA deposition is compared with that in 0.2 and 2.0*M* $Ni(NO_3)_2$ in Fig. 6. The deposition rate for the solution saturated in NO_3^- is approximately 75% of that in 0.2*M* $Ni(NO_3)_2$, indicating that the deposition rate is more dependent on the Ni(II) concentration than on the NO_3^- concentration. The 25% decrease in rate resulting from saturated NO_3^- may be an ionic strength effect.

The role of solution pH was also considered. Deposited mass was measured in 0.2*M* $Ni(NO_3)_2$ acidified to pH 3.0, 2.5, 2.0, and 1.5 and in 2.0*M* $Ni(NO_3)_2$ basified to pH 4.0.

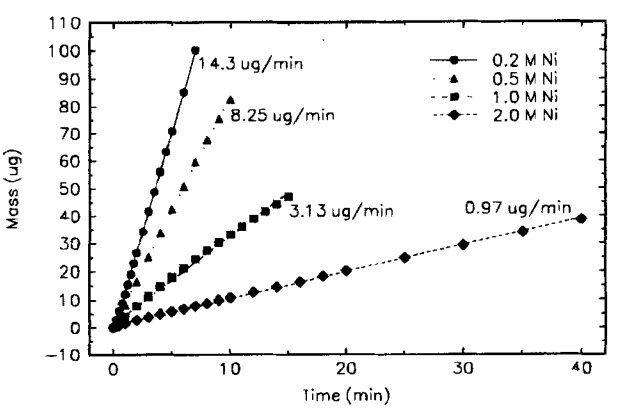

Fig. 5. A plot of mass *vs.* time at 0.5 mA in various $Ni(NO_3)_2$ concentrations. Note that the rate of deposition increases dramatically with decreasing solution concentration. The deposition rates at each concentration are indicated on the figure.

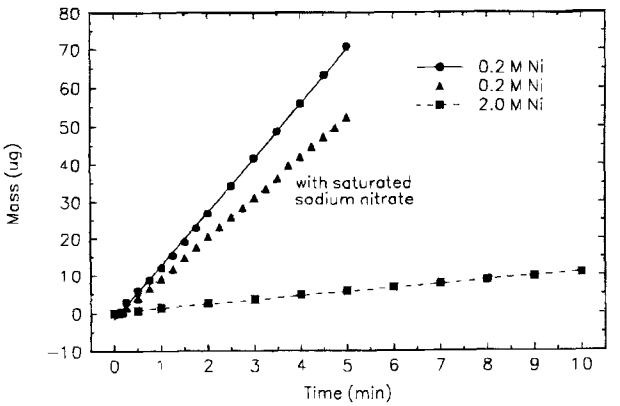

Fig. 6. A comparison of the mass *vs.* time data for 0.2*M* $Ni(NO_3)_2$, 2.0*M* $Ni(NO_3)_2$, and a 0.2*M* $Ni(NO_3)_2$ solution saturated with $NaNO_3$. The deposition rate of the solution saturated with NO_3^- is approximately 75% of that in 0.2*M* $Ni(NO_3)_2$.

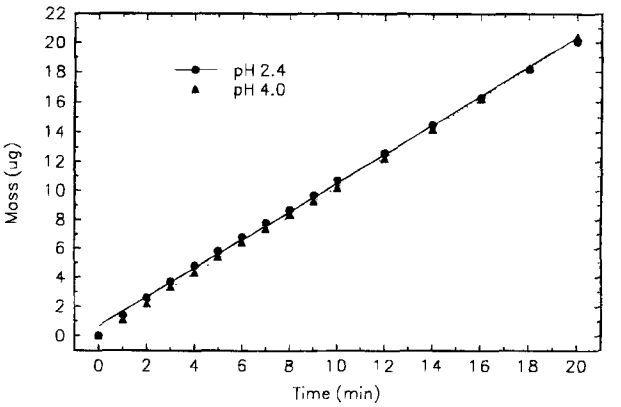

Fig. 8. A plot of mass *vs.* time for deposition in basified 2.0*M* $Ni(NO_3)_2$. The deposition rate is unchanged at a pH of 4.0.

The effect of pH in 0.2*M* $Ni(NO_3)_2$ is shown in Fig. 7. Acidification to pHs of 3.0, 2.5, and 2.0 decreases the deposition rate by less than 10%. Not until the pH was lowered to 1.5 was the deposition rate significantly diminished. However, even at that low pH the deposition rate was nearly an order of magnitude greater than that in 2.0*M* $Ni(NO_3)_2$ (in which the pH is approximately 2.4). Regarding the 2.0*M* $Ni(NO_3)_2$ solution, increasing the pH to 4.0 did not change the rate of deposition as shown in Fig. 8. Based upon the results shown in Fig. 7 and 8 it can be concluded that the rate of $Ni(OH)_2$ deposition is nearly independent of pH in the typical pH range of these solutions (pH 2 to 5) and that the concentration effects observed are not the result of pH.

The relationship between deposition rate at an applied current of 0.5 mA and $Ni(NO_3)_2$ concentration is illustrated in Fig. 9, which plots the deposition rate with respect to the inverse of concentration. The horizontal dashed line shows a theoretical deposition rate at which 100% of the electrochemically produced OH^- is utilized in the deposition of $Ni(OH)_2$. According to Eq. 1 and Faraday's law, the horizontal line is given as follows

$$\frac{dm}{dt} = \frac{9iAM_{Ni(OH)_2}}{16F} \qquad [3]$$

where dm/dt is the deposition rate (g/s), i is the applied current density (A/cm^2), A is the electrode area (0.2 cm^2), $M_{Ni(OH)_2}$ is the molecular weight of $Ni(OH)_2$ (for the purpose of this work we assumed a value of 93 g/mol which neglects codeposition of H_2O) and the 9/16 (as opposed to 9/8) indicates that 2 mols of hydroxyl are needed for the deposition of 1 mol of $Ni(OH)_2$. Note that Eq. 3 predicts that mass increases linearly with time and that mass is independent of solution concentration. It can be seen in Fig. 9 that at low $Ni(NO_3)_2$ concentrations (0.2 and, especially, 0.1*M*) nearly 100% of the generated OH^- is consumed in the deposition of $Ni(OH)_2$. However, at higher $Ni(NO_3)_2$ concentrations the efficiency of OH^- utilization decreases dramatically (to less than 20% at solution concentrations greater than 1.0*M*). Further, at high concentrations the rate of deposition is shown to be linearly related to the inverse of the solution concentration (with a regression value, R^2, of 0.997). This type of behavior was observed over a range of one order of magnitude of current (0.1 to 1.0 mA).

The data at different applied currents can be normalized by plotting the utilization efficiency of the electrochemically generated OH^- *vs.* inverse concentration as illustrated in Fig. 10. Note that the efficiency of utilization, while increasing slightly with current, is relatively independent of the deposition current. At all currents the utilization is highly inefficient in concentrated solutions and nearly 100% efficient in dilute solutions. It is clear from Fig. 10 that an empirical correlation can be developed to predict the mass of $Ni(OH)_2$ if the deposition conditions (time, current and solution concentration) are known. Since the data are linearly related to the inverse concentration in concentrated solutions and asymptotically approach 100% utilization of the electrochemically generated OH^- in dilute solutions an expression of the following form can be used

$$y = \{[y_1(x)]^n + [y_2(x)]^n\}^{1/n} \qquad [4]$$

where $y_1(x)$ and $y_2(x)$ are functions that fit the data at high and low concentrations, respectively, and n is adjusted to fit the asymptotic region. The slope of the line at the high

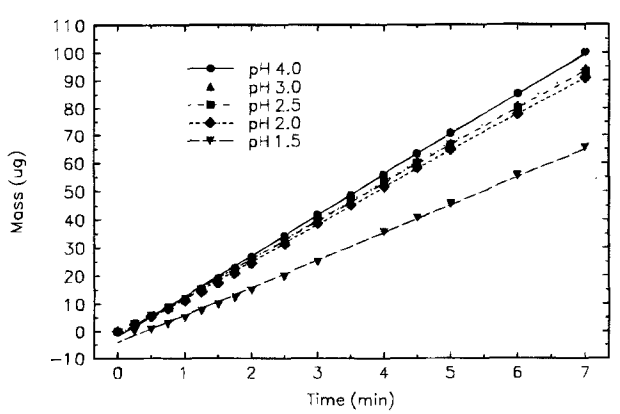

Fig. 7. A plot of mass *vs.* time for deposition in acidified 0.2*M* $Ni(NO_3)_2$. Acidification to pHs of 3.0, 2.5, and 2.0 decreases the deposition rate by less than 10%.

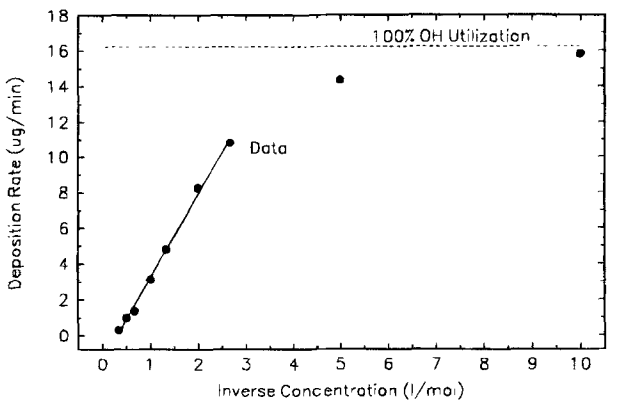

Fig. 9. A plot of deposition rate at 0.5 mA *vs.* inverse $Ni(NO_3)_2$ concentration. The horizontal dashed line shows a theoretical deposition rate predicted by Faraday's law. The deposition rate is observed to be both highly inefficient and linearly related to inverse concentration in concentrated solutions.

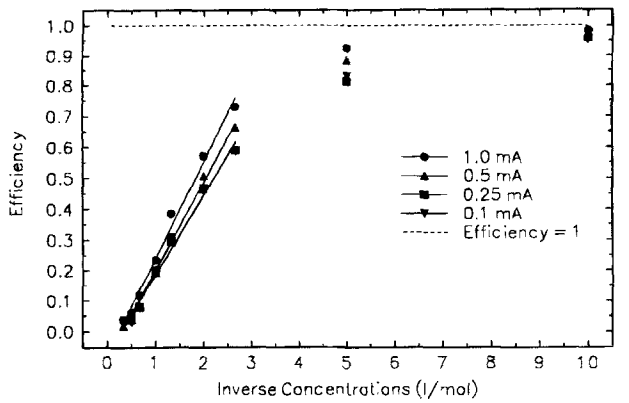

Fig. 10. A plot of the utilization efficiency of electrochemically generated OH^- *vs.* inverse $Ni(NO_3)_2$ concentration. The efficiency is relatively independent of current. At all currents utilization of OH^- is highly inefficient in concentrated solutions and nearly 100% efficient in dilute solutions.

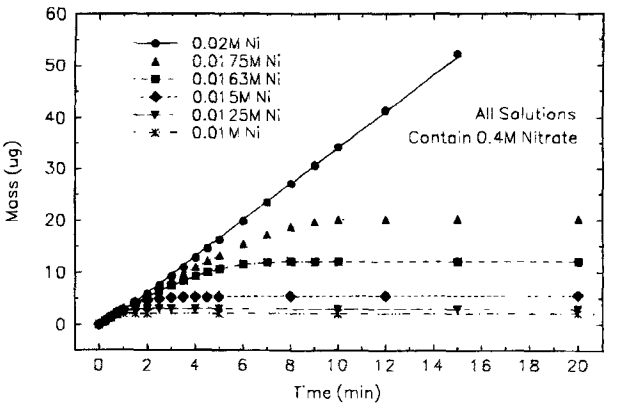

Fig. 12. A plot of mass *vs.* time at 0.1 mA in highly dilute $Ni(NO_3)_2$ solutions (<0.2*M*). Deposition stops after a short time. The mass at which deposition stops is a strong function of $Ni(NO_3)_2$ concentration, indicating a mass transport limitation of nickel.

concentration limit has approximately a linear relationship with current. Substituting in expressions for $y_1(x)$ and $y_2(x)$ derived from Fig. 10 and choosing a value of n that fits the asymptotic region of the 1.0 mA data yields the following expression

$$\epsilon_{OH^-} = \left[\left(\frac{0.321 - 0.015(5.0 - i)}{C_{Ni(NO_3)_2}} - 0.065\right)^{-3.5} + 1.0\right]^{-\frac{1}{3.5}} \quad [5]$$

where ϵ_{OH^-} is the efficiency of utilization of the electrochemically generated OH^-, $C_{Ni(NO_3)_2}$ is the concentration of the $Ni(NO_3)_2$ bath, and i is the applied current density in units of mA/cm^2. Note that the slope of efficiency *vs.* inverse concentration observed in concentrated solutions has been given a small dependence on applied current as observed in Fig. 10. ϵ_{OH^-} is then used as a multiplier in Eq. 3 to determine deposited mass. This is expressed in Eq. 6

$$\frac{dm}{dt} = \frac{9iAM_{Ni(OH)_2}\epsilon_{OH^-}}{16F} \quad [6]$$

Figure 11 shows the data from Fig. 10 fitted to Eq. 5 at deposition currents of 0.1 and 1.0 mA. As can be seen in the figure, the fit provides a prediction of utilization efficiency, and therefore deposition rate, within 10% of the measured value at all concentrations and currents.

It is important to note that Eq. 5 and 6 are not valid under all deposition conditions, but only under those reported in this study. Those conditions are as follows: first, the deposition experiments reported here were all performed at room temperature (23 to 25°C). Many impregnation recipes suggest elevated temperatures (>50°C).[1] However, at low concentrations, where ϵ_{OH^-} is approximately 1, the correlation may hold even at elevated temperatures. Second, Eq. 5 and 6 have been shown to hold over one order of magnitude of applied current (0.1 to 1.0 mA or 0.5 to 5.0 mA/cm^2). Third, all depositions were from solutions consisting of a 50/50 v/o mixture of ethanol and water. Finally, the range of concentrations in which Eq. 5 is valid is dependent on the deposition current. At 1.0 and 0.5 mA the correlation is only valid down to 0.1*M*. However, at 0.1 mA the correlation is valid to 0.02*M*.

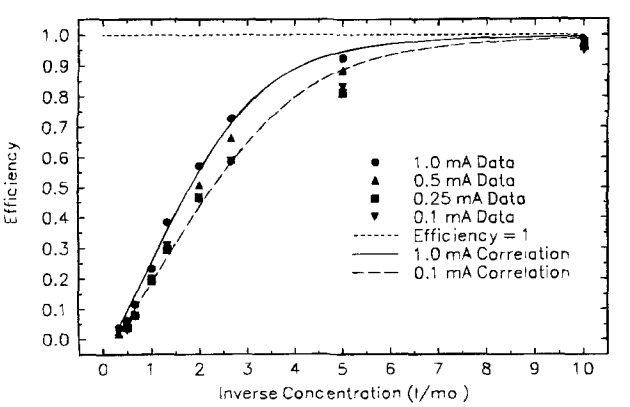

Fig. 11. The data from Fig. 10 fitted to the empirical correlation given in Eq. 4 and 5. The fit is shown to be good over the range of concentrations and currents used in this study.

The deposition behavior at 0.1 mA in dilute solutions (<0.02*M*) is shown in Fig. 12. After a short time, the deposition essentially shuts off, as indicated by the plateau in the mass-time curve. Further, it is shown in Fig. 12 that the mass at which deposition shuts off is a strong function of the solution concentration, decreasing with decreasing concentration. Three regions of interest are evident in the mass-time curves. Initially the slopes are identical at all concentrations with the value equivalent to that predicted by Faraday's law (see Eq. 3). Once the initial surface region becomes depleted the rate decreases and becomes limited by the mass transfer of Ni^{++} to the reaction interface. Eventually the deposition shuts off as the pH boundary moves away from the electrode surface (because the rate of OH^- generation is faster than its consumption by $Ni(OH)_2$ deposition) and precipitation occurs in the bulk.

It has been shown above that the increased NO_3^- concentration and the decreased pH in concentrated $Ni(NO_3)_2$ solutions are not the primary causes of the inefficient utilization of OH^-. The mechanism must therefore be related to the increased Ni(II) concentration in solution. Nickel is well known to complex in aqueous solutions, forming various soluble species (*e.g.*, $NiOH^+$, $Ni(OH)_2(aq)$, $Ni(OH)_3^-$, and $Ni(OH)_4^{2-}$ [25]). Perrin[26] demonstrated that Ni^{++} is in equilibrium with $NiOH^+$ in dilute solutions. Other researchers (see references in Baes and Mesmer[25]) have shown that the predominant species in more concentrated Ni(II) solutions (>0.015*M*) is the polymeric $Ni_4(OH)_4^{4+}$. Equilibrium is given by Eq. 7

$$4Ni^{++} + 4OH^- \leftrightarrow Ni_4(OH)_4^{4+} \quad [7]$$

where $\log K_{eq} = 28.3$. In the pH range of the bulk $Ni(NO_3)_2$ solutions used in this study (2.4 to 4.0), Eq. 7 indicates that the concentration of $Ni_4(OH)_4^{4+}$ is negligible ($<10^{-11}M$). However, in the pH range where deposition of $Ni(OH)_2$ begins (neutral pH; see Eq. 2) the concentration of $Ni_4(OH)_4^{4+}$ is similar to that of Ni^{++}. Baes and Mesmer[25] conclude that "small amounts of the polynuclear species $Ni_4(OH)_4^{4+}$ form rapidly at high Ni(II) concentrations (over 0.1*M*) before precipitation of $Ni(OH)_2$ occurs."

From the equilibrium expressions given in Eq. 2 and 7 the equilibrium concentration of $Ni_4(OH)_4^{4+}$ at the pH at which deposition begins can be calculated. The equilibrium constants for Eq. 2 and 7 can be expressed as follows

$$K_{sp} = c_1c_2^2 \quad [8]$$

$$K_{13} = \frac{c_3}{c_1^4 c_2^4} \quad [9]$$

where c_1, c_2, and c_3 are the concentrations of Ni^{++}, OH^-, and $Ni_4(OH)_4^{4+}$, respectively. Substituting Eq. 8 into 9 yields

$$\frac{c_3}{c_1^2} = K_{13}K_{sp}^2 = 5.1 \quad [10]$$

If we assume that Ni^{++} and $Ni_4(OH)_4^{4+}$ are the dominant species in solution, the following also holds

$$c_1 + 4c_3 = c_4 \quad [11]$$

where c_4 is the concentration of $Ni(NO_3)_2$ added to the solution. Equations 10 and 11 can be solved simultaneously, for c_1 and c_3 using the known $Ni(NO_3)_2$ concentrations. Table I gives the equilibrium values for the concentration of Ni^{++} and $Ni_4(OH)_4^{4+}$ as well as the pH at which deposition begins for each of the solution concentrations used in this study.

Based upon the above discussion, the following two-step deposition mechanism is proposed for high $Ni(NO_3)_2$ concentrations. First, Ni^{++} combines with OH^- to form $Ni_4(OH)_4^{4+}$ according to Eq. 7. The $Ni_4(OH)_4^{4+}$ then combines with more OH^- to form deposited $Ni(OH)_2$ as given in Eq. 12

$$Ni_4(OH)_4^{4+} + 4OH^- \rightarrow 4Ni(OH)_2\downarrow \quad [12]$$

Depending on the deposition conditions, $Ni_4(OH)_4^{4+}$ either reacts with the OH^- and deposits as $Ni(OH)_2$, according to Eq. 12, or it diffuses away from the electrode. If there is significant diffusion away from the electrode, deposition rates will be less than that predicted by Faraday's law. Since the concentration of $Ni_4(OH)_4^{4+}$ is essentially equal to zero in the acidic environment of the bulk solution, the concentration gradient of $Ni_4(OH)_4^{4+}$ is proportional to its concentration near the electrode surface. In concentrated $Ni(NO_3)_2$ solutions, where the concentration of $Ni_4(OH)_4^{4+}$ is high at the electrode (see Table I), the diffusion of $Ni_4(OH)_4^{4+}$ away from electrode will be rapid. This process consumes OH^- and decreases the efficiency of utilization of electrochemically generated OH^-. Decreasing the concentration of $Ni(NO_3)_2$ from 1.0 to 0.1*M* decreases the concentration of $Ni_4(OH)_4^{4+}$ at the electrode surface by a factor of 15 (from 0.20 to 0.013*M*) and hence the diffusion of this species. The net result is an increase in the rate of deposition by a factor of 5.

Conclusions

An electrochemical quartz crystal nanobalance (EQCN) has been utilized to measure the mass of $Ni(OH)_2$ films electrochemically deposited from $Ni(NO_3)_2$ solutions. The electrochemical deposition of $Ni(OH)_2$ has been quantified with respect to deposition time, current, and $Ni(NO_3)_2$ concentration. The mass changes measured via the EQCN were demonstrated to be the result of $Ni(OH)_2$ deposition. Cyclic voltammograms of the deposited material showed the characteristic charge and discharge peaks indicating the presence of the $Ni(OH)_2$/NiOOH couple while the charge passed in galvanostatic discharges were consistent with the masses determined via the EQCN.

The deposited mass was observed to increase proportionally with both time and current. Most significantly, however, the deposition rate was found to decrease significantly with increasing $Ni(NO_3)_2$ concentration. At low concentrations (*e.g.*, 0.2 or 0.1*M*) it was demonstrated that the utilization efficiency of electrochemically generated OH^- was nearly 100%. At high concentrations (*e.g.*, 1.0 or 2.0*M*) the utilization efficiency of OH^- was significantly less than 100% [approximately 20% in 1.0*M* $Ni(NO_3)_2$] and linearly related to the inverse $Ni(NO_3)_2$ concentration. The effect of concentration was shown to be related to Ni as opposed to solution pH or NO_3^- concentration. An empirical correlation was obtained which quantified deposition rates in solutions ranging from 0.1 to 3.0*M* $Ni(NO_3)_2$ and at current densities ranging from 0.5 to 5.0 mA/cm^2. The inefficient utilization of OH^- in concentrated $Ni(NO_3)_2$ is attributed to the formation of $Ni_4(OH)_4^{4+}$, which diffuses away from the reaction interface before deposition occurs.

Table I. The equilibrium concentrations of Ni^{++} and $Ni_4(OH)_4^{4+}$ at the electrode surface and the pH at which deposition begins in the $Ni(NO_3)_2$ concentrations used in this study. These values are obtained by solving Eq. 9-13. Note that the concentration of $Ni_4(OH)_4^{4+}$ is a strong function of the concentration of $Ni(NO_3)_2$. The bulk concentration of $Ni_4(OH)_4^{4+}$ in the acidic $Ni(NO_3)_2$ is essentially zero ($<10^{-11}$ M).

$[Ni(NO_3)_2]$ (*M*)	$[Ni^{++}]$ (*M*)	$[Ni_4(OH)_4^{4+}]$ (*M*)	pH
0.10	0.049	0.013	7.8
0.20	0.077	0.031	7.7
0.375	0.11	0.066	7.6
0.50	0.13	0.092	7.5
0.75	0.17	0.15	7.5
1.0	0.20	0.20	7.5
1.5	0.25	0.31	7.4
2.0	0.29	0.43	7.4
3.0	0.36	0.66	7.3

Acknowledgments

The authors acknowledge financial support from the Office of Research and Development of the United States Central Intelligence Agency for this project. The authors also acknowledge Mark Hines for valuable discussions regarding aqueous nickel chemistry.

Manuscript submitted July 18, 1994; revised manuscript received Nov. 10, 1994.

The University of South Carolina assisted in meeting the publication costs of this article.

REFERENCES

1. S. Gross, *Review of Electrochemical Impregnation for Nickel Cadmium Cells*, Jet Propulsion Laboratory, California Institute of Technology, Pasadena, CA (1977).
2. H. N. Seiger and V. J. Puglisi, *Proc. of the 26th Power Sources Symposium*, Atlantic City, NJ, p. 115 (1974).
3. D. F. Pickett and J. T. Maloy, *This Journal*, **125**, 1026 (1978).
4. K. Ho, *ibid.*, **134**, 52C (1987).
5. K. Ho and J. Jorné, *ibid.*, **137**, 149 (1990).
6. F. Portemer, A. Delahaye-Vidal, and M. Figlarz, *ibid.*, **139**, 671 (1992).
7. P. K. Ng and E. W. Schneider, *ibid.*, **133**, 17 (1986).
8. D. A. Corrigan and R. M. Bendert, *ibid.*, **136**, 723 (1989).
9. M. Paszkiewicz, *J. Appl. Electrochem.*, **11**, 443 (1981).
10. M. W. Earl and T. F. Noble, *J. Power Sources*, **12**, 277 (1984).
11. W. Fischer, *Electrochim. Acta*, **21**, 1001 (1976).
12. D. M. MacArthur, *ibid.*, **117**, 730 (1970).
13. D. A. Corrigan, *ibid.*, **134**, 377 (1987).
14. J. Desilvestro, D. A. Corrigan, and M. J. Weaver, *ibid.*, **135**, 885 (1988).
15. D. A. Corrigan and S. L. Knight, *ibid.*, **136**, 613 (1989).
16. R. M. Bendert and D. A. Corrigan, *ibid.*, **136**, 1369 (1989).
17. P. Bernard, C. Gabrielli, M. Keddam, H. Takenouti, J. Leonardi, and P. Blanchard, *Electrochim. Acta*, **33**, 743 (1991).
18. S. I. Cordoba-Torresi, C. Gabrielli, A. Hugot-Le Goff, and R. Torresi, *This Journal*, **138**, 1548 (1991).
19. I. C. Faria, R. Torresi, and A. Gorenstein, *Electrochim. Acta*, **38**, 2765 (1993).
20. J. W. Weidner and P. Timmerman, *This Journal*, **141**, 346 (1994).
21. S. Motupally, C. C. Streinz, and J. W. Weidner, *ibid.*, In press.
22. *Technical Manual, Electrochemical Quartz Crystal Nanobalance*, System EQCN-500, Elchema, Potsdam, NY.
23. V. J. Puglisi, H. N. Seiger, and D. F. Picket, in *Proceedings of the 9th IECEC*, p. 873, American Chemical Society, Washington, DC (1974).
24. D. F. Picket, H. H. Rogers, L. A. Tinker, C. A. Bleser, J. M. Hill, and J. S. Meador, in *Proceedings of the 15th IECEC*, p. 1918, American Chemical Society, Washington, DC (1980).
25. C. F. Baes and R. E. Mesmer, *The Hydrolysis of Cations*, pp. 242-247, John Wiley & Sons, New York (1976).
26. D. D. Perrin, *J. Chem. Soc.*, 3644 (1964).